

Highly Conducting π -Conjugated Molecular Junctions Covalently Bonded to Gold Electrodes

Wenbo Chen,[†] Jonathan R. Widawsky,[‡] Héctor Vázquez,[‡] Severin T. Schneebeli,[†] Mark S. Hybertsen,^{*,§} Ronald Breslow,^{*,†} and Latha Venkataraman^{*,‡}

Departments of [†]Chemistry and [‡]Applied Physics and Applied Mathematics, Columbia University, New York, New York 10027, United States

[§]Center for Functional Nanomaterials, Brookhaven National Laboratory, Upton, New York 11973-5000, United States

S Supporting Information

ABSTRACT: We measure electronic conductance through single conjugated molecules bonded to Au metal electrodes with direct Au–C covalent bonds using the scanning tunneling microscope based break-junction technique. We start with molecules terminated with trimethyltin end groups that cleave off *in situ*, resulting in formation of a direct covalent σ bond between the carbon backbone and the gold metal electrodes. The molecular carbon backbone used in this study consist of a conjugated π system that has one terminal methylene group on each end, which bonds to the electrodes, achieving large electronic coupling of the electrodes to the π system. The junctions formed with the prototypical example of 1,4-dimethylenebenzene show a conductance approaching one conductance quantum ($G_0 = 2e^2/h$). Junctions formed with methylene-terminated oligophenyls with two to four phenyl units show a 100-fold increase in conductance compared with junctions formed with amine-linked oligophenyls. The conduction mechanism for these longer oligophenyls is tunneling, as they exhibit an exponential dependence of conductance on oligomer length. In addition, density functional theory based calculations for the Au–xylylene–Au junction show near-resonant transmission, with a crossover to tunneling for the longer oligomers.

It is a great challenge to achieve electronically transparent connections between metal electrodes and organic molecules,¹ so as to minimize resistance introduced by the chemical linkers normally used to form such interfaces.² Typically, thiols^{2b,3} that bind covalently to gold, or amines^{2a,b,4} that form donor–acceptor bonds to under-coordinated gold, are used to electronically couple organic backbones to metal electrodes. For each link group, analysis of a series of single-molecule junctions as a function of length has generally revealed a large contact resistance, significantly larger than the ideal limit for a single channel of one conductance quantum ($G_0 = 2e^2/h$).^{2a,c,5} A junction with conductance close to G_0 has been demonstrated for H_2 and benzene molecules with platinum electrodes under high-vacuum conditions at low temperatures.^{2d,6} However, the ability to create and control transport through highly conducting molecular–metal interfaces remains a major challenge, especially under ambient conditions.

We have shown previously that direct Au–C covalent σ bonds can be created *in situ* at the molecule–gold interface, resulting in

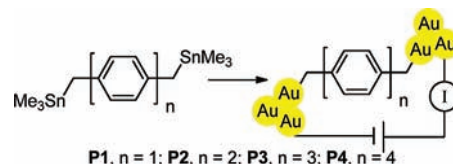


Figure 1. *In situ* formation of direct Au–electrode–C bonds starting from $SnMe_3$ precursors.

highly conducting σ -bonded systems.⁷ For example, a conductance of $0.1 G_0$ through a butane backbone was demonstrated. These direct Au–C bonded molecular junctions were created starting with trimethyltin-terminated alkanes. The trimethyltin end-groups cleave off *in situ*, yielding direct Au–C bond coupled junctions. Our density functional theory (DFT)-based calculations showed that, in the limit of a single methylene group, a conductance approaching G_0 could be achieved, suggesting that the direct Au–C link has near-ideal transmission characteristics. While we succeeded in forming junctions with benzene, the conductance was relatively low, consistent with calculations indicating conduction occurred through the σ system.^{7,8}

Here, we create single-molecule junctions using conjugated backbones terminated with methylene groups that bind covalently to gold metal electrodes, again through the use of $SnMe_3$ groups that cleave off *in situ*. We find that the resulting junctions have a conductance that is 100-fold higher than those of similar junctions formed with conventional linkers.⁹ These junctions are highly conducting because the Au–C bonds to the terminal methylene units are well coupled to the conjugated π system. This is in contrast to similar junctions created previously, where Au was bound directly to a carbon on the benzene ring.⁷ Specifically, we find that the conductance of *p*-xylylene bonded to gold electrodes approaches $1 G_0$. Our theoretical calculations show that conduction occurs via near-resonant transmission. For longer polyphenyls with 2–4 phenyl units, we find that the conductance decreases exponentially with increasing length, with a characteristic decay constant of 1.9/phenyl group.

We synthesized a series of trimethylstannylmethyl-terminated polyphenyls and measured the conductance of single-molecule junctions formed from these molecules using the scanning tunneling microscope based break-junction (STM-BJ) method (Figure 1).^{2a,3b} In this technique, single-molecule junctions are

Received: August 24, 2011

Published: September 22, 2011

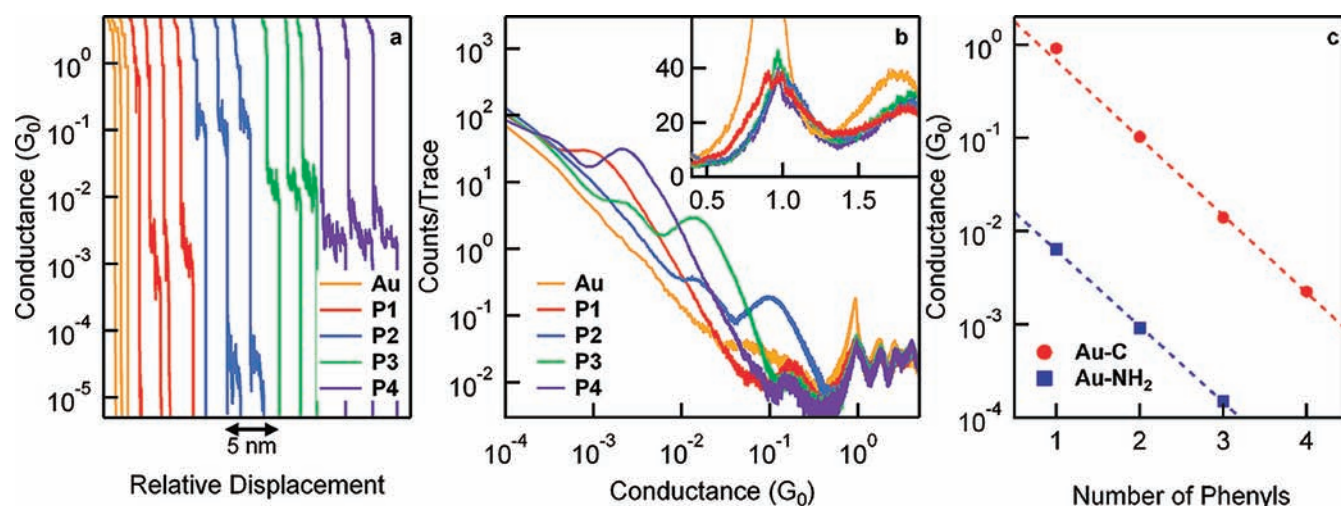


Figure 2. (a) Individual conductance traces measured in solutions of the SnMe₃-terminated polyphenyl compounds P1–P4. Measurements in solvent alone are also shown for comparison (Au). The applied bias is 250 mV. (b) Conductance histograms of over 10 000 traces generated with linear bin size of 0.0001 G_0 , shown on a log–log scale. Inset: the same data on a linear scale. (c) Conductance versus number of phenylene units in the chain for P1–P4, and analogous measurements with a diamine series taken from ref 12. Dotted lines represent linear least-squares fit to P2–P4 series. Note the point for P1 above the line.

created by repeatedly forming and breaking Au point contacts^{3b} in a ~ 10 mM 1,2,4-trichlorobenzene solution of the target trimethyltin-terminated molecules. Conductance (current/voltage) is measured as a function of the relative tip/sample displacement to yield conductance traces, which are used to generate conductance histograms. We synthesized 1,4-trimethylstannyl-terminated xylylene using two different methods. In one, we converted 1,4-bis-bromomethylbenzene (*p*-xylylene dibromide) to the dilithio compound and reacted it with trimethylstannyl chloride.¹⁰ In the other method, we reacted the *p*-xylylene dibromide with trimethylstannyl lithium.¹¹ The latter procedure was used to attach the trimethylstannyl groups for the polyphenyl compounds. The details of these synthetic procedures and characterizations are given in the Supporting Information (SI). We note here that these compounds are toxic and should be handled with care.

Figure 2a compares individual conductance traces from measurements of solutions of stannylated 1,4-dimethylenebenzene, 4,4'-dimethylenebiphenyl, 4,4''-dimethylene-*p*-terphenyl, and 4,4'''-dimethylene-*p*-tetrphenyl (P1, P2, P3, and P4, respectively). We see clear conductance plateaus at molecule-dependent conductance values, although in the case of P1 it is not straightforward to distinguish the molecular plateau from that of the single-atom contact at a conductance around G_0 . These plateaus are due to conduction through a molecule bonded in the gap between the two Au point-contacts. These conductance plateaus are seen in the measurements immediately after a solution of the target molecule terminated with SnMe₃ groups is added, in contrast with measurements of 1,4-bis(trimethylstannyl)-benzene,⁷ where conductance plateaus were seen in measurements only after 2.5 h. This delay seen in measurements of 1,4-bis(trimethylstannyl)-benzene indicated that conduction did not occur through trimethylstannyl terminated molecules. In our past work,⁷ this was confirmed by showing that the conductance of auryltriphenylphosphine terminated compounds were the same as those terminated by SnMe₃ groups.

In addition to plateaus seen at a high conductance, the traces in Figure 2a show a second series of plateaus at 0.001 G_0 for P1 (red) and 3×10^{-5} G_0 for P2 (blue). These are attributed to

in situ dimerization of the target compounds after the SnMe₃ linkers have been lost on the gold electrodes, in which the conjugated systems are linked by a dimethylene bridge. Indeed, some traces show two plateaus, one due to the monomer and one from the dimer. However, we cannot determine, on the basis of conductance alone, whether both are present during the entire measurement. We will return to these features later in this paper.

Repeated measurements give a statistical assessment of the junction properties. In Figure 2b, we show conductance histograms for each of the compounds studied here. Each conductance histogram, generated from over 10 000 traces without any data selection, reveals clear peaks at conductance values that depend on the molecular backbone. The inset of Figure 2b shows the same conductance histograms on a linear scale around 1 G_0 . Here, we see a clear peak around 0.9 G_0 for P1 that can be distinguished from the peak near 1 G_0 that is due to the conductance through a single gold-atom contact. By fitting the peaks in these conductance histograms with Lorentzians, we determine that the conductance of P1 is about 0.9 G_0 , while the values for P2, P3, and P4 are 0.1 G_0 , 0.014 G_0 , and 0.0022 G_0 , respectively. The position of the highest conductance peak in each histogram is plotted on a semilog scale against the number of phenyl rings in the molecule in Figure 2c. We find that, for the series P2–P4, the conductance decays exponentially with increasing number of phenyl groups, with a decay constant $\beta = 1.9/\text{phenyl}$ or 0.43/Å. For comparison, in Figure 2c, we also plot the conductance of polyphenyls doubly terminated with amine linkers, which show a similar decay in conductance with length.¹²

The histogram for P1, in Figure 2b, also shows a peak around 0.001 G_0 due to the presence of dimer molecules formed *in situ* during the measurement. To show that this is indeed due to conduction through a dimer molecule, we synthesized the dimer precursor of *p*-xylylene dimer (P1d, see Figure 3a) and measured its conductance in the STM-BJ setup. The conductance histogram for P1d shows a clear peak at 0.001 G_0 but no feature other than the gold conductance peak at 1 G_0 (SI Figure 1). This clearly demonstrates that the dimer molecule P1d is created *in situ* when measurements of P1SnMe₃ are carried out. That the conductance

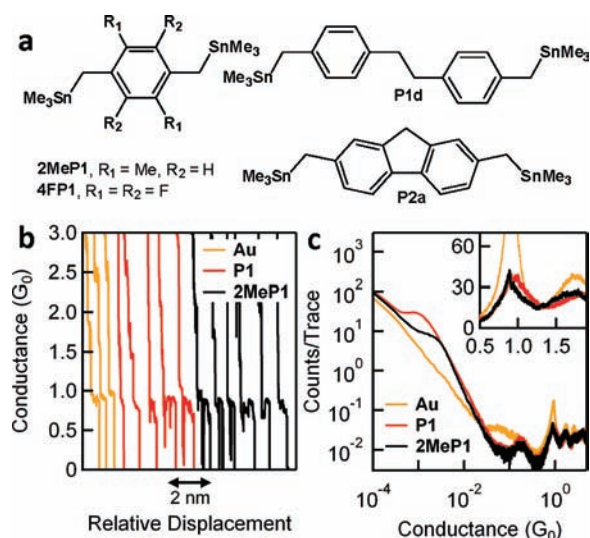


Figure 3. (a) Structures of additional compounds studied. (b) Individual conductance traces measured in solutions of the SnMe₃-terminated compounds **P1** (red) and **2MeP1** (black) at 25 mV applied bias. (c) Conductance histograms of over 10 000 individual measurements, generated with linear bin size of 0.0001 G₀, shown on a log–log scale. Inset: same histograms on a linear scale.

of the dimer is almost 3 orders of magnitude lower than that of the monomer can be attributed to the saturated dimethylene bridge between the two conjugated parts.

We also synthesized and measured the conductances of two xylylene derivatives with trimethyltin terminations (see SI for details). The first is a dimethyl-substituted xylylene (**2MeP1**), and the second is a tetrafluoro-substituted xylylene (**4FP1**) (Figure 3a). For **2MeP1**, we see a conductance peak at ~0.9 G₀, very close to that of the unsubstituted **P1**, as shown in Figure 3c. The fact that the methyl substituents do not affect conductance significantly is consistent with a near-resonant transport mechanism, as will be discussed further below. Thus for both **P1** and **2MeP1**, we demonstrate near-resonance transport across a molecular junction 0.8 nm in length.

The histogram for **2MeP1** in Figure 3c also shows a second peak around 0.002 G₀, due to the formation of the dimer molecule, as in the case of **P1**. However, here we see a change in the conductance of the **P1** dimer when compared with that of the **2MeP1** dimer, as we expect when the mechanism for transport involves tunneling through the saturated ethano group. In contrast to the results with **2MeP1**, we find that **4FP1** does not show clear evidence for junction formation. The conductance histogram generated from 10 000 measurements does not show two clear peaks around G₀ or a peak due to the molecular dimer formed *in situ* (SI Figure 2). We attribute this to a stronger Sn–C bond in **4FP1SnMe₃**, making *in situ* cleavage of the SnMe₃ group more difficult.

In our past work with Au–C coupled alkanes and benzene,⁷ we found that the conductance of 1,4-didehydrobenzene covalently bonded to Au electrodes was only 0.03 G₀, significantly lower than that of *p*-xylylene. For benzene, only the molecular σ system, which is a rather poor conductor, was well coupled through the Au–C bonds.^{7,8} In contrast, with xylylene the Au–C bonds are very well coupled to the π system, yielding the high conductances observed. In principle, this coupling will depend on the angle between the Au–C bond and the phenyl plane and will be maximum when this angle is 90°.¹³ On the basis of

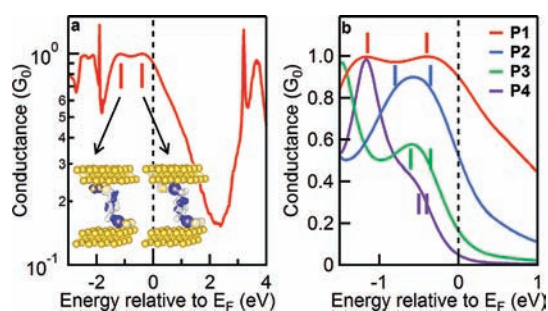


Figure 4. (a) Calculated transmission spectrum for **P1** bonded to Au electrodes. Inset: isosurface plots of the real part of the transmitted scattering states for energies at the vertical bars (–1.15 and –0.4 eV), showing the even and odd combinations of the Au–C bonds coupled through the π backbone. (b) Transmission spectra for **P1**–**P4**. Bars indicate the approximate position Au–C MO energies.

calculations for this system, we find indeed that the minimum energy configuration has a 90° angle, and the barrier for rotation is 10.4 kcal/mol, or 0.45 eV (SI Figure 4).

The conductance of **P2**, the biphenyl analogue of **P1**, is 0.10 G₀ (Figure 2b). This conductance is a factor of 9 lower than that of **P1**, while in the case of amine-terminated polyphenyls, the difference between benzene and biphenyl was a factor of only ~6. To see if the difference between **P1** and **P2** is partly due to an anomalous internal twist angle at the central C–C bond, we synthesized a trimethyltin-terminated analogue of fluorene with two methylene groups (**P2a**) and measured its conductance using the STM-BJ setup. We find that **P2a** has a conductance of 0.17 G₀ (SI Figure 3), but the conductance ratio between **P1** and **P2a** (5.3) is still larger than the ratio for the diamine analogues (4.3).⁹ This indicates that the lower conductance of an Au–**P2**–Au junction compared with that of the Au–**P2a**–Au junction partly reflects a twist in the phenyl–phenyl bond that is absent in the fluorene analogue. However, we see that an Au–**P1**–Au junction still has a higher conductance than one would expect, just extrapolating the exponential dependence seen for the longer polyphenyl compounds investigated here.

To understand the origin of the high conductance observed in these junctions, we carried out DFT-based first-principles calculations¹⁴ with a gradient-corrected exchange–correlation functional¹⁵ and a nonequilibrium Green’s function approach¹⁶ to calculate electronic transmission through these junctions (see SI for details). Transmission curves for **P1**–**P4** junctions are shown in Figure 4. The calculated zero-bias conductances are 0.9 G₀, 0.5 G₀, 0.15 G₀, and 0.05 G₀ for **P1**–**P4**, respectively. Transmission at the Fermi level is derived from the molecular orbitals (MOs) on the Au–C bonds that are very well coupled to the molecular π backbone and to the gold electrodes. For **P1**, this results in two distinct resonances, one for an even combination of the Au–C bond MOs and one for the odd combination, as seen from the isosurface plots of the transmitted scattering state for each resonance (Figure 4a).¹⁷ Physically, the Au–C bond MOs and the nearby π backbone MOs are nominally fully occupied by electrons. The extent to which the Fermi level for this junction falls within the nearest resonance depends on the amount of charge transfer from the molecule to the electrodes. An analysis of the Mulliken populations for the **P1** junction shows net positive charge, with the molecule having lost about 0.5 electron. The electrostatic balance leads to the Fermi energy being placed slightly above the highest MO resonance, resulting in conductance of **P1** being near-resonant, with a magnitude close to G₀.

For the longer derivatives, the effective through- π -system coupling between the Au–C MOs is reduced. The corresponding energy splitting between the even and odd combinations of these MOs also gets smaller, and the two distinct resonances seen for **P1** merge into a single, broad feature at ~ -0.5 eV, with decreased transmission at the peak (Figure 4b). However, the distinct even and odd combinations of the Au–C MOs can still be clearly seen in the transmitted scattering states (SI Figures 5–7). The charge transfer from the molecule to the electrodes is similar to that for **P1**, and the Fermi level is pinned at an energy just above the highest resonance. The computed decay constant β for **P2–P4** is 1.2/phenyl group.

There are inherent errors in the use of the DFT MOs and energies for transport calculations in nanoscale junctions.¹⁸ While the impact is minor for cases where the junction conductance is close to G_0 , e.g., for metal point contacts,¹⁹ the calculated conductance values in the tunneling regime for single-molecule junctions are typically larger than those measured in experiment.^{18d,f,20} In the present case, we expect that corrections to the DFT-based theory will only change the **P1** transmission modestly, leaving a resonance with near-unit transmission close to the Fermi energy. However, the DFT-calculated π backbone MO energy is likely too close to the Fermi energy in general, an effect that will be larger for longer oligomers, where screening by the electrodes becomes less effective. In this case, the conductance will be smaller than indicated by the DFT calculations, with an increase in the effective β value for **P2–P4**.

In conclusion, we have demonstrated a clear method to create circuits with strong electronic coupling between gold electrodes and conjugated molecules. We achieve a single-molecule junction conductance close to one quantum across a length of ~ 0.8 nm. This remarkable result opens up new methods to create long and highly conducting molecular junctions.

■ ASSOCIATED CONTENT

S Supporting Information. Synthetic procedures, measurement details, additional data, and computational details. This material is available free of charge via the Internet at <http://pubs.acs.org>.

■ AUTHOR INFORMATION

Corresponding Author

rb33@columbia.edu; mhyberts@bnl.gov; lv2117@columbia.edu

■ ACKNOWLEDGMENT

This work was supported in part by the Nanoscale Science and Engineering Initiative of the NSF (award CHE-0641523), the New York State Office of Science, Technology, and Academic Research (NYSTAR), and NSF Career Award CHE-07-44185 (L.V.). J.R.W. was supported by the EFRC program of the U.S. Department of Energy (DOE) under Award No. DE-SC0001085. S.T.S. was the recipient of a Guthikonda Graduate Chemistry Fellowship. Part of this work was carried out at the Center for Functional Nanomaterials, Brookhaven National Laboratory, which is supported by the DOE Office of Basic Energy Sciences, under contract no. DE-AC02-98CH10886.

■ REFERENCES

(1) (a) Nitzan, A.; Ratner, M. A. *Science* **2003**, *300*, 1384. (b) Joachim, C.; Ratner, M. A. *PNAS* **2005**, *102* (25), 8801.

- (2) (a) Venkataraman, L.; Klare, J. E.; Tam, I. W.; Nuckolls, C.; Hybertsen, M. S.; Steigerwald, M. L. *Nano Lett.* **2006**, *6*, 458. (b) Chen, F.; Li, X. L.; Hihath, J.; Huang, Z. F.; Tao, N. J. *J. Am. Chem. Soc.* **2006**, *128*, 15874. (c) Park, Y. S.; Whalley, A. C.; Kamenetska, M.; Steigerwald, M. L.; Hybertsen, M. S.; Nuckolls, C.; Venkataraman, L. *J. Am. Chem. Soc.* **2007**, *129*, 15768. (d) Kiguchi, M.; Tal, O.; Wohlthat, S.; Pauly, F.; Krieger, M.; Djukic, D.; Cuevas, J. C.; van Ruitenbeek, J. M. *Phys. Rev. Lett.* **2008**, *101*, 046801. (e) Martin, C. A.; Ding, D.; Sorensen, J. K.; Bjornholm, T.; van Ruitenbeek, J. M.; van der Zant, H. S. J. *J. Am. Chem. Soc.* **2008**, *130*, 13198. (f) Schneebeli, S. T.; Kamenetska, M.; Cheng, Z.; Skouta, R.; Friesner, R. A.; Venkataraman, L.; Breslow, R. *J. Am. Chem. Soc.* **2011**, *133*, 2136. (g) Mishchenko, A.; Zotti, L. A.; Vonlanthen, D.; Burkle, M.; Pauly, F.; Cuevas, J. C.; Mayor, M.; Wandlowski, T. *J. Am. Chem. Soc.* **2011**, *133*, 184. (h) Kosov, D. S.; Li, Z. Y. *J. Phys. Chem. B* **2006**, *110*, 9893. (i) von Wrochem, F.; Gao, D. Q.; Scholz, F.; Nothofer, H. G.; Nelles, G.; Wessels, J. M. *Nat. Nanotechnol.* **2010**, *5*, 618.
- (3) (a) Reed, M. A.; Zhou, C.; Muller, C. J.; Burgin, T. P.; Tour, J. M. *Science* **1997**, *278*, 252. (b) Xu, B. Q.; Tao, N. J. *Science* **2003**, *301*, 1221. (c) Haiss, W.; Wang, C. S.; Grace, L.; Batsanov, A. S.; Schiffrin, D. J.; Higgins, S. J.; Bryce, M. R.; Lambert, C. J.; Nichols, R. J. *Nat. Mater.* **2006**, *5*, 995.
- (4) Kiguchi, M.; Miura, S.; Takahashi, T.; Hara, K.; Sawamura, M.; Murakoshi, K. *J. Phys. Chem. C* **2008**, *112*, 13349.
- (5) (a) Beebe, J. M.; Engelkes, V. B.; Miller, L. L.; Frisbie, C. D. *J. Am. Chem. Soc.* **2002**, *124* (38), 11268–11269. (b) Li, X. L.; He, J.; Hihath, J.; Xu, B. Q.; Lindsay, S. M.; Tao, N. J. *J. Am. Chem. Soc.* **2006**, *128* (6), 2135–2141. (c) Li, C.; Pobelov, I.; Wandlowski, T.; Bagrets, A.; Arnold, A.; Evers, F. *J. Am. Chem. Soc.* **2008**, *130* (1), 318–326.
- (6) Smit, R. H. M.; Noat, Y.; Untiedt, C.; Lang, N. D.; van Hemert, M. C.; van Ruitenbeek, J. M. *Nature* **2002**, *419*, 906.
- (7) Cheng, Z. L.; Skouta, R.; Vazquez, H.; Widawsky, J. R.; Schneebeli, S.; Chen, W.; Hybertsen, M. S.; Breslow, R.; Venkataraman, L. *Nat. Nanotechnol.* **2011**, *6*, 353.
- (8) Ma, G. H.; Shen, X.; Sun, L. L.; Zhang, R. X.; Wei, P.; Sanvito, S.; Hou, S. M. *Nanotechnology* **2010**, *21* (49), 495202.
- (9) Venkataraman, L.; Klare, J. E.; Nuckolls, C.; Hybertsen, M. S.; Steigerwald, M. L. *Nature* **2006**, *442*, 904.
- (10) Cohen, T.; Bhupathy, M. *Acc. Chem. Res.* **1989**, *22*, 152.
- (11) (a) Still, W. C. *J. Am. Chem. Soc.* **1979**, *101*, 2493. (b) Still, W. C. *J. Am. Chem. Soc.* **1978**, *100*, 1481.
- (12) Hybertsen, M. S.; Venkataraman, L.; Klare, J. E.; Whalley, A. C.; Steigerwald, M. L.; Nuckolls, C. *J. Phys.: Cond. Mat.* **2008**, *20*, 374115.
- (13) Park, Y. S.; Widawsky, J. R.; Kamenetska, M.; Steigerwald, M. L.; Hybertsen, M. S.; Nuckolls, C.; Venkataraman, L. *J. Am. Chem. Soc.* **2009**, *131*, 10820.
- (14) Soler, J. M.; Artacho, E.; Gale, J. D.; Garcia, A.; Junquera, J.; Ordejon, P.; Sanchez-Portal, D. *J. Phys.: Cond. Mat.* **2002**, *14*, 2745.
- (15) Perdew, J. P.; Burke, K.; Ernzerhof, M. *Phys. Rev. Lett.* **1996**, *77*, 3865.
- (16) Brandbyge, M.; Mozos, J. L.; Ordejon, P.; Taylor, J.; Stokbro, K. *Phys. Rev. B* **2002**, *65*, 165401.
- (17) Paulsson, M.; Brandbyge, M. *Phys. Rev. B* **2007**, *76*.
- (18) (a) Toher, C.; Filippetti, A.; Sanvito, S.; Burke, K. *Phys. Rev. Lett.* **2005**, *95*, 4. (b) Evers, F.; Weigend, F.; Koentopp, M. *Phys. Rev. B* **2004**, *69*. (c) Neaton, J. B.; Hybertsen, M. S.; Louie, S. G. *Phys. Rev. Lett.* **2006**, *97*, 216405. (d) Ke, S. H.; Baranger, H. U.; Yang, W. T. *J. Chem. Phys.* **2007**, *126*, 201102. (e) Sai, N.; Zwolak, M.; Vignale, G.; Di Ventra, M. *Phys. Rev. Lett.* **2005**, *94*. (f) Thygesen, K. S.; Rubio, A. *Phys. Rev. B* **2008**, *77*. (g) Thygesen, K. S.; Rubio, A. *Phys. Rev. Lett.* **2009**, *102*.
- (19) (a) Darancet, P.; Ferretti, A.; Mayou, D.; Olevano, V. *Phys. Rev. B* **2007**, *75*, 075102. (b) Calzolari, A.; Di Felice, R.; Manghi, F. *Phys. Rev. B* **2005**, *72*.
- (20) (a) Quek, S. Y.; Choi, H. J.; Louie, S. G.; Neaton, J. B. *Nano Lett.* **2009**, *9*, 3949. (b) Quek, S. Y.; Venkataraman, L.; Choi, H. J.; Louie, S. G.; Hybertsen, M. S.; Neaton, J. B. *Nano Lett.* **2007**, *7*, 3477. (c) Strange, M.; Rostgaard, C.; Hakkinen, H.; Thygesen, K. S. *Phys. Rev. B* **2011**, *83*.